Solid Freeform Fabrication 2023: Proceedings of the 34th Annual International Solid Freeform Fabrication Symposium – An Additive Manufacturing Conference
Reviewed Paper

Benchmarking the Tensile Properties of Polylactic Acid (PLA) Recycled Through Fused Granule Fabrication Additive Manufacturing

Dawood Al Nabhani*, Ali Kassab†, Osama Habbal*, Pravansu Mohanty*, Georges Ayoub†, and Christopher Pannier*
*Department of Mechanical Engineering, University of Michigan – Dearborn, MI 48128
†Department of Industrial and Manufacturing Systems, University of Michigan – Dearborn, MI 48128

Abstract

To progress toward a circular economy of thermoplastic polymers, the adoption of 3D printers to make functional articles can facilitate distributed recycling. To this end, the mechanical degradation of polymers through multiple recycling cycles must be quantified. This work presents a procedure and benchmark dataset of tensile property degradation for polylactic acid (PLA) feedstock in multiple recycling passes with a fused granule fabrication process. To establish recycling with minimal processing (shredding and sieving), modifications were required to the granule feeding hopper of the 3D printer. Two distinct orientations were chosen to obtain tensile test coupons. These coupons were die-cut from machined 3D printed rectangular cross-section tubes, with one orientation along the bead (0°) and the other perpendicular to it (90°). Tensile properties are presented for 3D printed virgin material and one, two, three, and four passes of recycling. In terms of print orientation, the results indicate that samples pulled at 0° and 90° exhibited similar mechanical properties. However, there was an average decrease of 3.1% in ultimate tensile strength and a 1.7% decrease in elastic modulus for the samples along 90° orientation for all recycling passes. The samples along 0° demonstrated a 13.7% higher strain at fracture compared to those along 90°. Regarding the number of recycling passes, the findings suggest that the mechanical characteristics of PLA remain largely unaffected even after undergoing four recycling cycles. However, when the material is pulled in the direction of the bead, a 3.09% decrease in ultimate tensile strength is observed in the fourth recycling pass. The elastic modulus and strain at fracture did not exhibit a clear trend. It is important to note that the testing results display some variability, which can be attributed to a combination of stochasticity in the printing process and the preparation procedure employed.

Keywords: Additive Manufacturing, Recycling, PLA

Introduction

The concept of circular economy (CE) in thermoplastic polymers has received global attention, including the proposed distributed recycling by additive manufacturing (DRAM) of thermoplastic polymers [1]. In particular, the fused granule fabrication (FGF) process holds great potential for DRAM by utilizing shredded feedstock and eliminating the requirement to produce a spooled filament with high tolerance [2]–[4]. The demand for distributed recycling is growing due to the projected increase in global waste generation. It is estimated to rise from 2.01 billion tons in 2016 to 2.59 billion tons in 2030 and further to 3.40 billion tons by 2050. Notably, 12%

of this waste consists of municipal plastic waste [5]. Therefore, open-source 3D printers are proliferating to give access to many users at all levels including individuals, community groups, and businesses to recycle thermoplastic waste at a local level [6],[7]. However, although recycling offers promise for creating a circular economy, it has its own limitations. First, for the purpose of mechanically recycling plastics, the material needs to be melted by significant motion of the chains. Polymers consist of various types of chains, and only thermoplastics, which are made up of linear chains, can be remelted. This limits the range of plastics that can be effectively mechanically recycled. Second, polymers experience degradation over time due to factors such as high temperatures, light exposure, moisture, humidity, or microorganisms. This degradation causes the material to lose its properties, reducing the likelihood of being recycled and meeting the necessary quality standards expected by the recycling community [8]. Polylactic acid (PLA) is a biodegradable semicrystalline polymer derived from biomass [9]. PLA has been widely used in various applications, particularly in consumer products, compostable products, and 3D printing filament, due to its favorable characteristics such as a low glass transition temperature and minimal shrinkage during 3D printing. Therefore, recyclability of PLA is of high interest. Thus, it is important to consider the mechanical properties of PLA, as they may undergo degradation after multiple recycling cycles [10]. Understanding the mechanical performance is crucial in determining the number of recycling passes before the material's mechanical integrity is compromised and it becomes unsuitable for producing products.

Although there is a rising interest in the recyclability of thermoplastic polymers in the field of 3D printing, prior investigations have predominantly prioritized mechanical recycling methodologies, with a particular emphasis on injection molding techniques [11]. Several studies explored the behavior and properties of 3D printed parts after multiple recycling passes. Cieslik et al. examined the effects of multiple reprocessing cycles on PLA with a conductive composite. They investigated variations in extrusion temperature and the number of recycling passes, observing a decline in thermal stability and material strength. During this investigation, instead of utilizing a 3D printer to extrude the filament, the material was broken down and melted at temperatures similar to those used for the material printing [12]. In their study, Tanney et al. aimed to evaluate how multiple extrusion cycles affect the properties of 3D printed parts and explore the feasibility of using a combination of new and recycled materials to maintain material integrity. To simulate the typical recycling process, the authors followed a three-stage approach. First, they pelletized the filament by feeding it into a chamber with a wood routing bit controlled by a drill press. Then, they recycled the filament by using a Filabot Original filament extruder to create a new filament. Finally, the recycled filament was used in the printing phase to create the 3D printed parts. The findings revealed a significant reduction in the strength, maximum strain, and toughness properties of the material due to the repeated heat cycles [13]. Anderson conducted an experiment using commercially available PLA and a basic 3D printer. They created and tested tensile and shear specimens to assess their ultimate tensile strength, elasticity, and hardness. The specimens were then recycled into filament using a Filabot EX2 and subjected to a second round of testing. The results showed that 3D printing with recycled PLA using the Filabot EX2 is a viable option. The recycled filament exhibited a slight decrease in tensile strength, an increase in shear strength, and a decrease in hardness. The tensile modulus of elasticity remained unchanged. However, the recycled filament showed more variability in the results compared to the virgin specimens [14].

An important aspect in 3D printing is anisotropic mechanical properties in a printed part. This is a well-established phenomenon often considered a drawback in additive manufacturing, especially in the fused filament fabrication (FFF) and fused granule fabrication (FGF) processes. Gradinaru et al. [15] found that PLA mechanical properties differed along the bead and perpendicular to it. However, the magnitude of the difference varies across different studies examining similar properties. Although there is an agreement that 3D printing materials exhibit direction-dependent mechanical properties, the specific results vary due to differences in sample preparation and the methodologies followed. For instance, in Alexandre et al.'s research [16], a substantial difference in tensile strength was observed between the 0° and 90° orientations, with the 0° orientation showing five times the strength of the 90° orientation. In another study, conducted by Grant et al. [17], the tensile strength was found to be twice as high in the 0° orientation compared to the 90° orientation. These works show that magnitude of anisotropy varies with printing and testing procedure.

The primary objective of this study is to quantitatively assess the degradation of PLA material after multiple recycling passes using FGF additive manufacturing process. By establishing a benchmark dataset that evaluates the degradation of tensile property degradation, this research aims to understand the PLA mechanisms of degradation as it undergoes additive manufacturing recycling across four iterations. To mitigate potential printing challenges arising from the use of recycled material, modifications were made to the feeding hopper of the GigabotX 2 XLT printer [18] incorporating an upgraded fluidized bed system to minimize occurrence of clogs while printing of the recycled passes.

Methodology

2.1 Material Preparation

In this study, LX175 virgin PLA pellets were sourced from a single supplier (Filabot) to ensure a consistent and standardized material with uniform properties. The pellets have an average diameter of 4.2 mm as shown in Figure 1 with a melting temperature range of 180-210° C [19]. To maintain consistency across the recycling passes, the granules were shredded repeatedly to achieve the same average diameter as the virgin pellets with 95% confidence level.

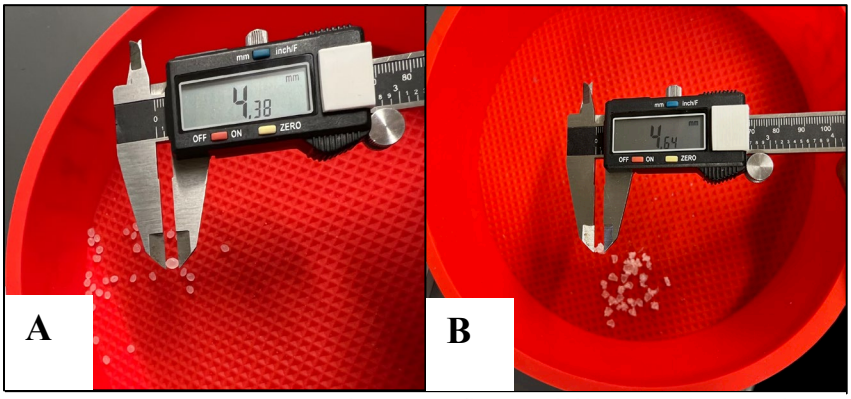

		Units	Mean	StDev	Minimum	Median	Maximum
A	**Virgin Pellets**	mm	4.2019	0.1796	3.8500	4.1900	4.5900
B	**Recycled Granules**	mm	4.2278	0.2318	3.5200	4.2500	4.6400

Figure 1: Determining the Size of the Virgin Pellets(A) and the Recycled Granules (B).

To investigate the mechanical degradation caused by multiple recycling passes, the virgin PLA was subjected to a series of recycling passes. Figure 2 presents an overview of the methodology used to produce the dog-bone specimens intended for testing purposes.

2.2 Recycling Process

The recycling process involved a series of steps, beginning with shredding, sieving, followed by drying, 3D printing, machining and finally punching along two different material directions (0°and 90°). These steps were designed to mimic real-world controlled recycling condition, enabling the process to be easily scaled for larger quantities of recycled material.

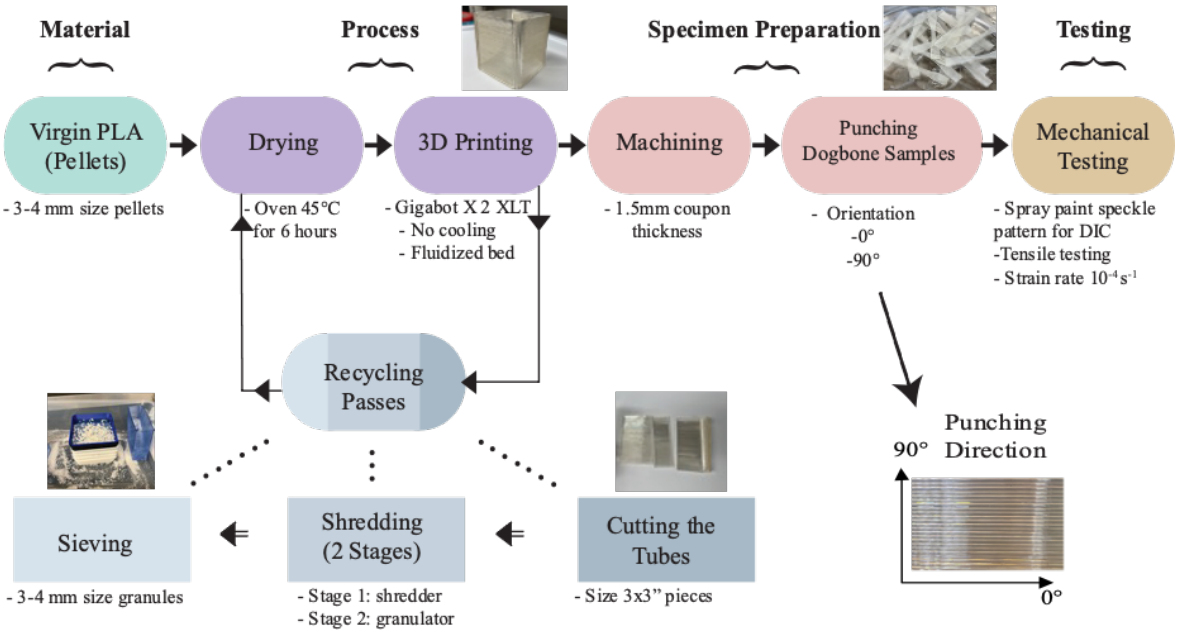

Figure 2: PLA Recycling Process

2.2.1 *Shredding*

The shredding process consisted of two stages. During the first one, the tubes were cut into 3 x 3 inches and fed into the shredder, resulting in granules sizes of approximately half an inch. In the second stage, the shredded PLA granules were subjected to multiple rounds of shredding, a process where they were repeatedly broken down into smaller pieces. This iterative shredding was carried out to continuously reduce the size of the PLA granules, making them more suitable for the printing process. The repeated shredding helped achieve the desired particle size for 3D printing. To maintain a contamination-free process, shredder was cleaned between each cycles using compressed air and hand tools.

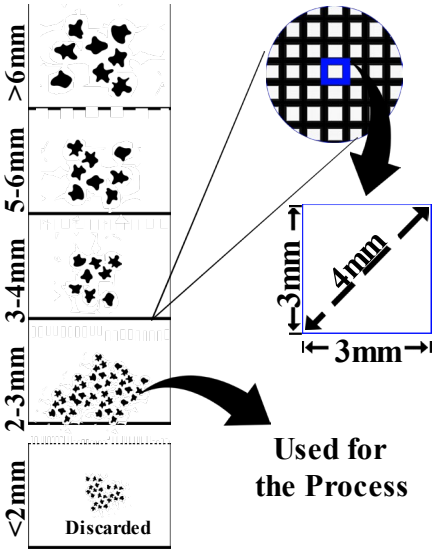

Figure 3 : Sieving System

2.2.2 *Sieving*

The Sieving process is an essential step for granules process. The purpose of this step is to segregate the shredded granules based on the size and use granules within the size of

3-4 mm as a feedstock to the 3D printer. To accomplish this requirement, a total of five sieves with different mesh sizes were utilized, classifying the granules into the following categories: >6mm ,5-6mm ,3-4mm, 2-3mm, <2mm. The arrangement and sequence of the sieving process can be observed in Figure 3. Any granules that exceeded the desired size were returned to the shredding system until they successfully pass through the 3-4mm sieve. Conversely, granules with a diameter smaller than 2mm were discarded.

2.2.3 *Drying*

The PLA material was dried by a conventional oven at a temperature of 45°C for a duration of 6 hours. This controlled drying process aimed to eliminate any moisture content in both the pellets and granules, thus ensuring optimal printing performance. Moreover, to enhance the preservation of the PLA material and minimize moisture absorption prior to printing, an additional precautionary measure was implemented by storing the material in a vacuum chamber.

2.2.4 *3D Printing*

A Gigabot X 2 XLT 3D printer was used to print the production square tubes represented by the CAD model in Figure 4.The tube was printed with the dimension of 80X80X100 mm (LxWxH) and a thickness of 3mm. This specific design was chosen to maximize the available wall surface area enabling the cutting of dog-bone shapes for tensile testing. Depending on the material direction along which the sample was extracted, whether 0° or 90°, each wall of the tube could yield approximately 5-6 dog-bone specimens.

Figure 4: 3D Printing Tubes

2.2.5 *Machining*

After the tubes were 3D printed, they were cut into four walls, followed by machining using an endmill from both sides to achieve a uniform thickness of 1.5mm, with tolerance of 1.47±0.09 mm. It is crucial to emphasize that ensuring flatness in the machined surfaces is of paramount importance. Any deviations in thickness can potentially affect the outcomes of the tensile tests. Therefore, strict control and thorough measurement of the flatness of all machined surfaces' thickness was carried out during this process. To provide visual insight, Figure 5 presents a cross-sectional view of a 3D printed tube wall, highlighting the bead patterns. The figure serves to illustrate the necessity of machining the tube walls to achieve the desired flatness and uniform thickness as well as to eliminate uneven edges, which might affect testing, as outlined in the research conducted by Cole et al.[15].

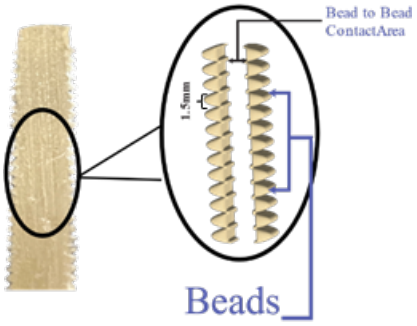

Figure 5: Cross-sectional View of a 3D Printed Tube Wall

2.3 Fluidized Bed for the Feeding System

In order to accommodate the 3D printing of recycled PLA granules, a modification was made to the feeding system of the GigabotX 2 XLT printer [18]. This modification was essential to ensure proper flow and uniform distribution of the recycled PLA granules during the additive manufacturing process. Figure 6 shows a detailed schematic of the fluidized bed system that was

designed specifically for the Gigabot X 2 XTL. The development of this upgrade was prompted by challenges encountered with clogging due to the irregular shape of the granules, which was expected in the recycling process. After numerous attempted alterations, the proposed modification demonstrated the highest success rate for achieving successful prints with granules. The system consists of a compressed air system delivering air at a constant rate of 3CFM and 115psi (gauge pressure), with the inlet controlled by a motorized ball valve that opens and closes based on the cycle showed in figure 7. Additionally, Figure 8 shows an image showcasing the installed fluidized bed system and presents the modified CAD design of the fluidized bed.

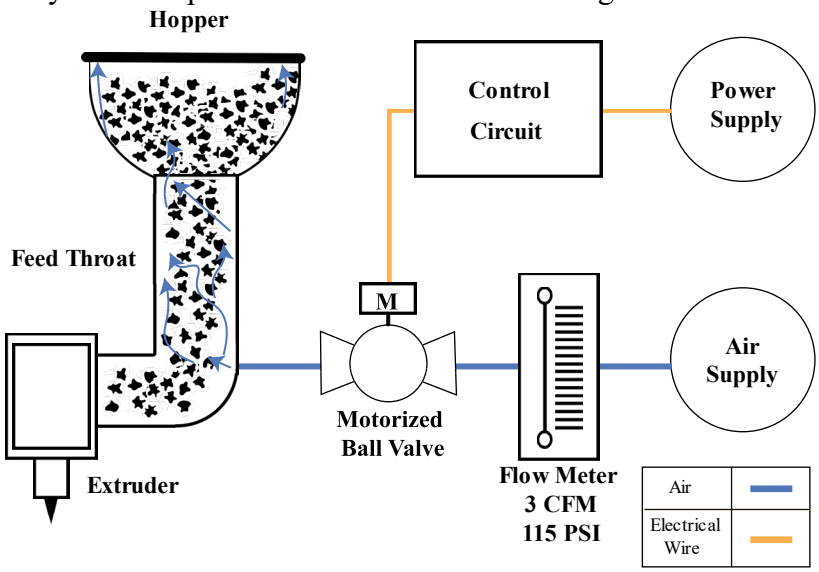

Figure 6: Fluidized Bed Schematic

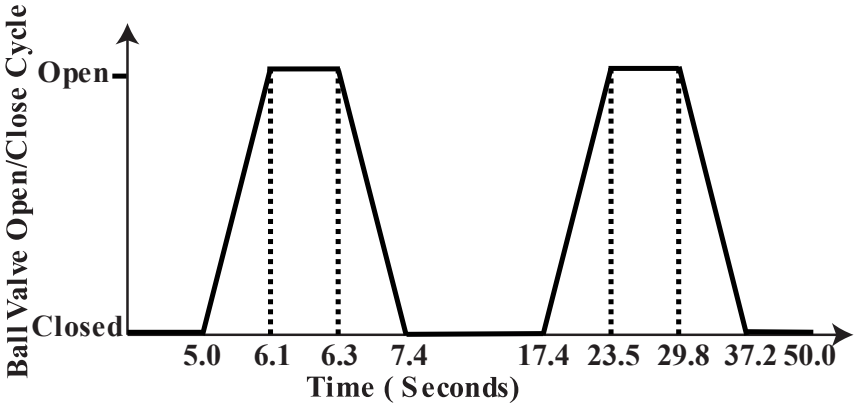

Figure 7: Ball Valve Opening and Closing Cycle

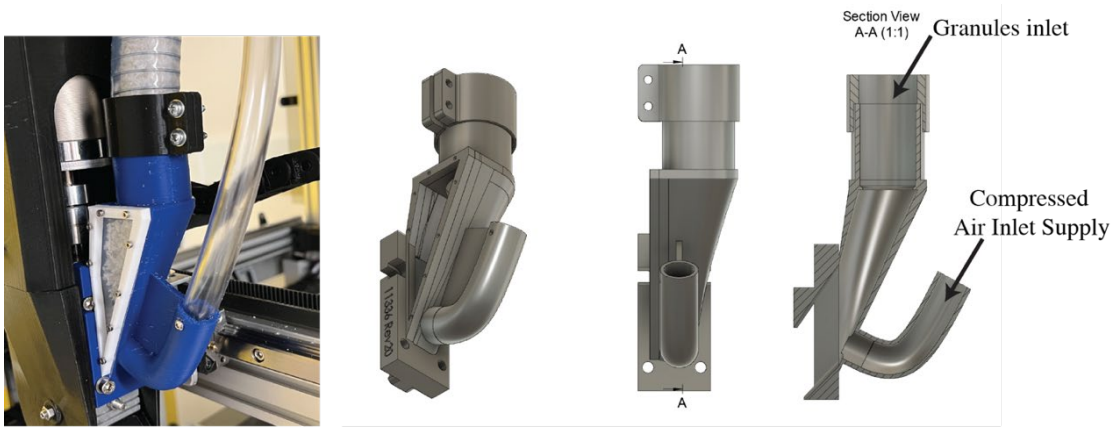

Figure 8: Photograph of the installed fluidized bed feed throat (A). Feed throat CAD design with section view (B).

2.4 Tensile Test Coupon Preparation

To ensure precise and accurate results, a procedure was developed to control the punching process. Figure 9 shows the septs used to punish the dog bone test specimens. The process involved using a manual press machine to punch out dog samples used for tensile testing. To facilitate the punching process, the 1.5mm sheet were heated in a convection oven at 50°C for 60 seconds. It is important to highlight the criticality of aligning the punching direction accurately. Two specific punching direction were used: 0° and 90° degrees, as clearly illustrated in Figure 2. The sheet was aligned either at 0°or 90° degrees from the reference bead, followed by the drawing of a precise straight line to guide the alignment of the dye cutter.

A non-standard dog-bone cutting die used was with a radius shape in the gauge area was selected. This test samples have a thinner middle section of the samples, increasing the likelihood of failure occurring at the center. A visual representation of the shape and geometry of the cutting die is provided in Figure 10.

The tensile properties of the 3D printed samples were assessed using the Instron E1000 mechanical testing system, which was equipped with a 1 KN load cell. Tensile tests were carried out at room temperature and using an engineering strain rate of $10^{-4}s^{-1}$.

To obtain the engineering stress-strain curves, the engineering stress was calculated by measuring the cross-sectional area of the specimen at its narrowest point, which is at the vertical center. The displacement was recorded from the software at the crosshead movement, and the engineering strain was determined using a gauge length of 43 mm, as shown in Figure 10. Figure 11 illustrates the Engineering stress-strain curve of the virgin sample for both the 0° and 90° orientation.

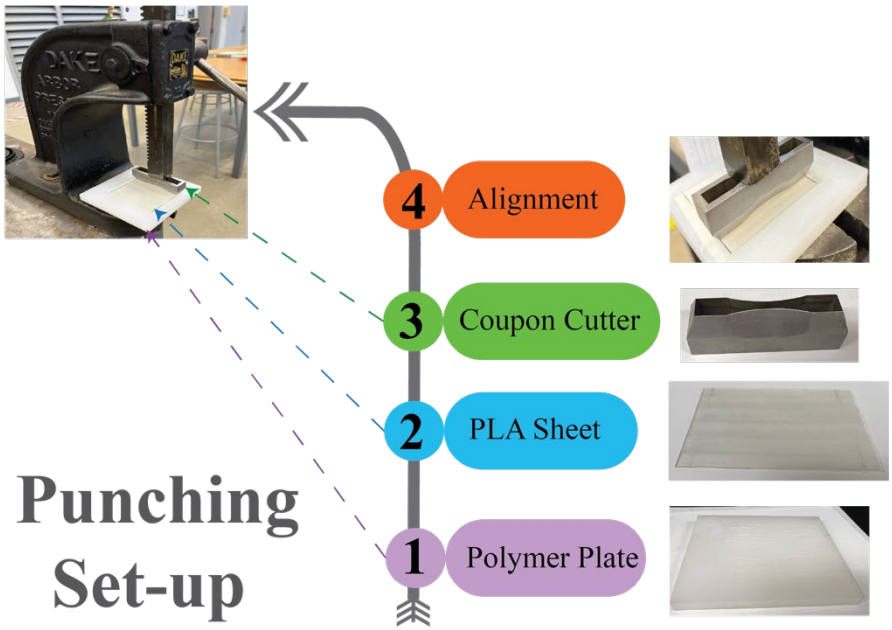

Figure 9: Punching set-up used for the experiment.

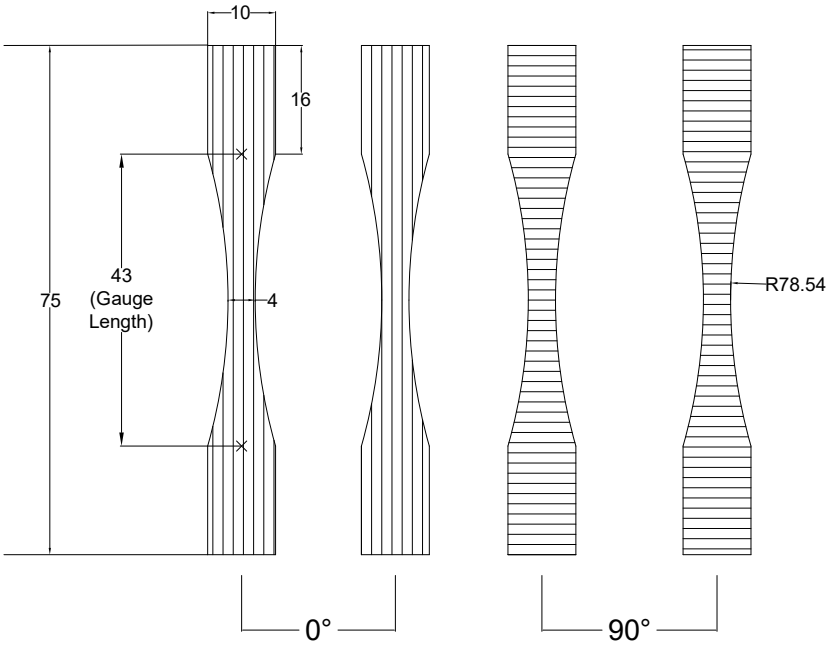

Figure10: Sample geometry and orientation, dimensions in mm. The gap between the lines in both orientations represents the bead thickness, which is equivalent to 1.5mm.

2.5 Additive Manufacturing/3D Printing Process

The Gigabot X 2 XTL printer [9] was used for the fused granule fabrication (FGF) process, which was utilized to produce the tubes. Both the virgin PLA material and the recycled PLA granules from each recycling pass were loaded separately into the granule feeding hopper of the printer. For slicing Simplify3D software was used, and the specific printing parameters are outlined in Table 1. Notably, fan cooling was not utilized during the printing process, and the maximum extrude cross-sectional area was optimized, increased from 7 to 12 mm^2.

Parameter	Value	Unit
Nozzle Diameter	2.85	mm
Layer Height	1.5	mm
Skirts Outlines	5	count
Bottom Heat Zone (T0)	185	ºC
Middle Heat Zone (T1)	180	ºC
Top Heat Zone (T2)	165	ºC
Bed Temperature	60	ºC
Printing Speed	900	mm/min
Travel Speed	6000	mm/min
Extrusion Multiplier	185	%
Layer time	30	seconds
Firmware Version (Klipper)	V0.10.0-297-gde1af3	
Firmware Setting; "max extrude cross section"	12	mm^2
Cooling Fan Speed	0	%
Slicer Software	Simplify3D	
3D Printer	Gigabot X 2 XLT	

Table 1: Printing Parameters

Results and Discussion

*3.1 Tensile Testing Method and Results*In the context of 3D printing, the layer-by-layer building process often leads to rounded edges and unfilled rectangular cross-sectional areas, resulting in a stepped surface appearance. To address this, machining techniques are utilized to eliminate these edges and achieve a smooth, flat surface for the final specimen geometry. Without machining, these imperfections may have been overlooked during the calculation of the cross-sectional area for tensile testing. Tensile testing was conducted on both virgin and recycled PLA samples, extracted along two material orientations. Our findings indicate that the print orientation does have a significant effect on yield strength when the specimens are subjected to tensile testing to failure. Our research specifically focuses on examining the adhesion and alignment of bead centers. Within our experimental design, we observed an average reduction of 3.12% in ultimate tensile strength and a 1.66% decrease in elastic modulus for the parts printed at a 90 degrees orientation. It is important to note that this decrease was not consistently observed across all recycling passes, which can be seen in the virgin and fourth recycled pass.

3.2 Property Degradation

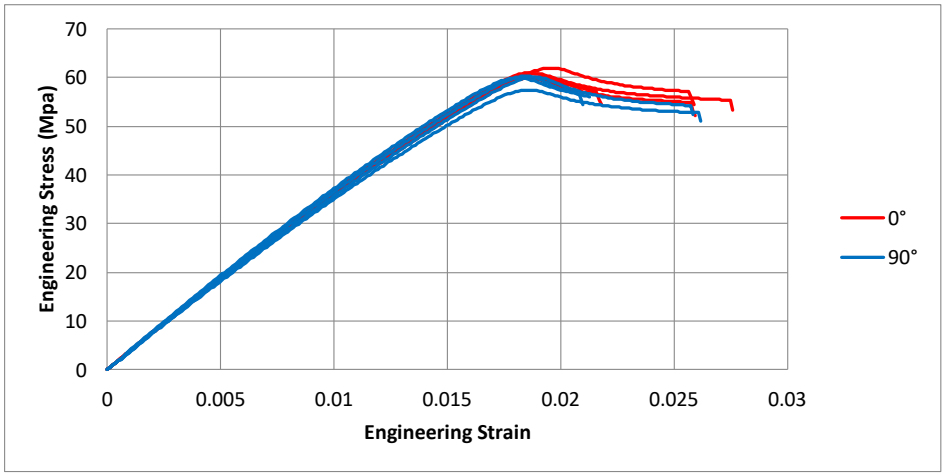

(a)

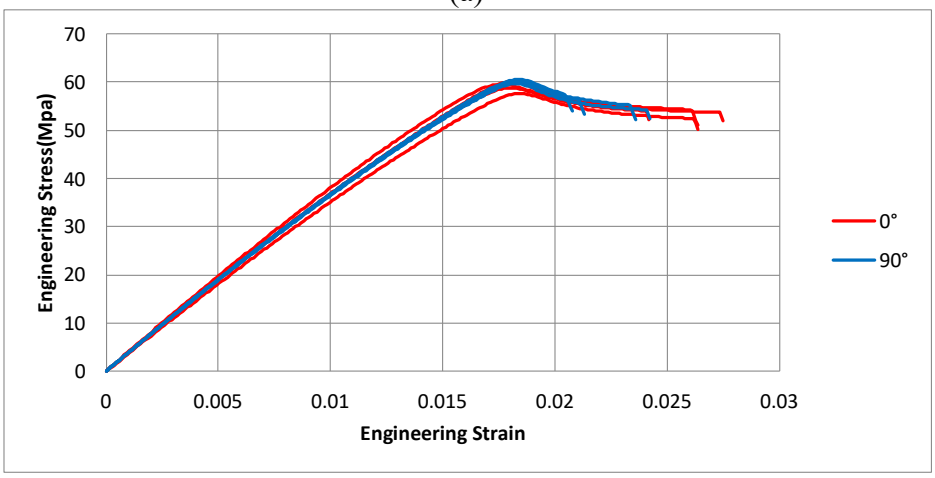

(b)

Figure 9: Stress Strain Curve corresponding to the Virgin (a) and 4th Recycling Pass (b) Prints for 0° and 90° Orientations

The recycling processes involved one, two, three, and four passes. The primary mechanical properties assessed encompassed ultimate tensile strength, elastic modulus, and strain at fracture.

Recycle Pass	Orientation	Ultimate Strength (MPa)	Elastic Modulus (MPa)	Strain at Fracture (%)
0	0	60.92 ± 0.87	3498.64 ± 044.55	2.52 ± 0.25
	90	59.48 ± 1.33	3489.17 ± 089.78	2.36 ± 0.28
1	0	60.56 ± 1.69	3613.74 ± 135.93	2.20 ± 0.10
	90	58.30 ± 1.49	3611.32 ± 071.65	2.15 ± 0.17
2	0	60.19 ± 1.64	3641.62 ± 067.65	2.20 ± 0.08
	90	56.21 ± 1.82	3522.81 ± 091.23	1.90 ± 0.16
3	0	61.68 ± 0.95	3559.64 ± 116.01	2.67 ± 0.30
	90	58.73 ± 1.23	3415.26 ± 091.41	2.08 ± 0.14
4	0	59.03 ± 1.08	3557.65 ± 118.62	2.61 ± 0.14
	90	60.14 ± 0.37	3534.66 ± 015.68	2.24 ± 0.17

Table 2: Mechanical properties of the tested samples over four recycling passes

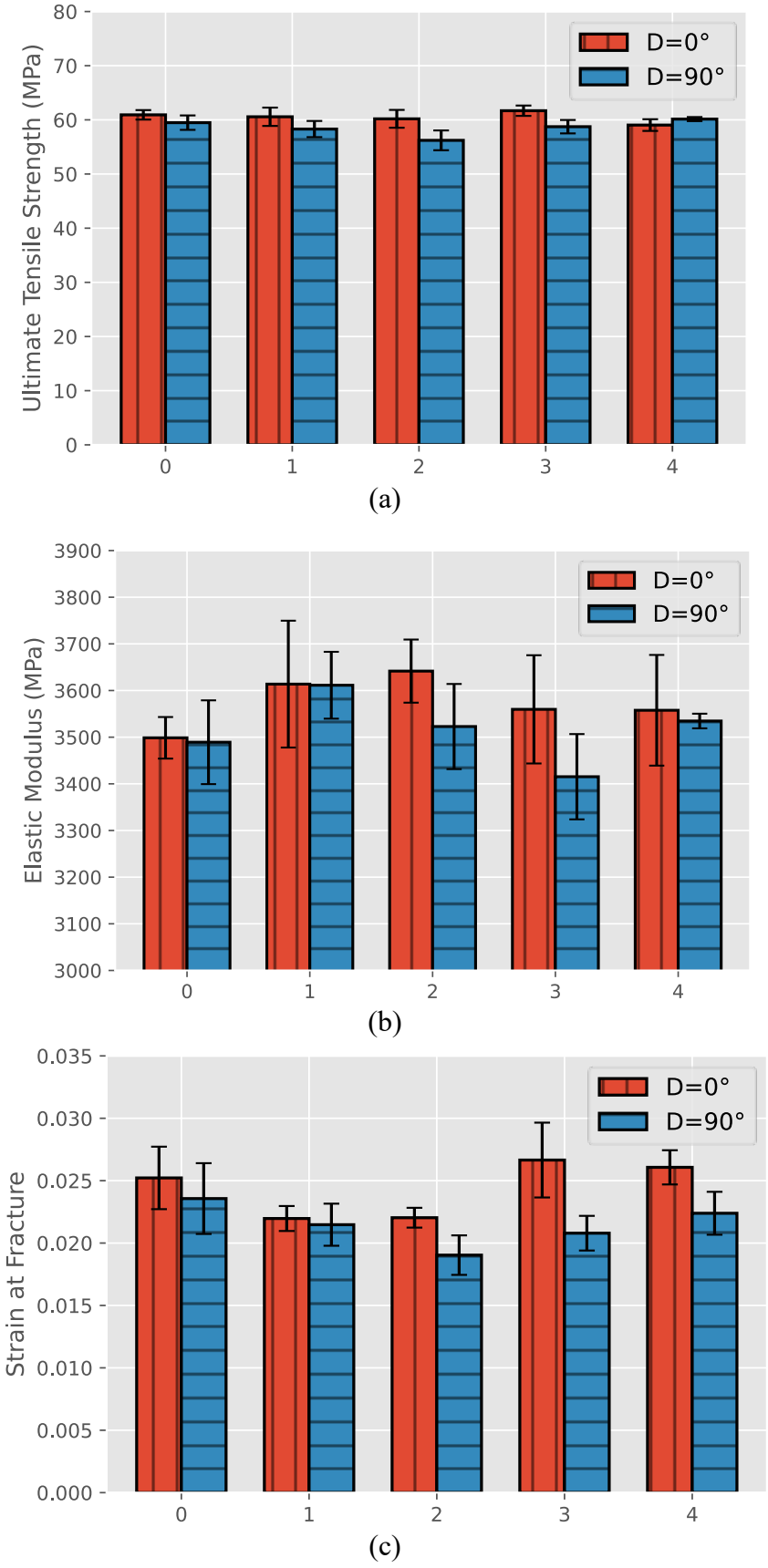

Figure 12: Ultimate Tensile Strength (a), Elastic Modulus (b) and Total Strain at Fracture (c) for Virgin and Four Recycling Processes ($\bar{x} \pm 2s_x$)

Figure 12 represents the ultimate tensile strength, elastic modulus, and strain at fracture, respectively. When comparing different print orientations, there was no evident pattern observed in the ultimate tensile strength or elastic modulus. However, it was consistently observed that samples with a 90° orientation tended to fracture earlier in comparison to samples with a 0° orientation. The samples printed at 90° demonstrated an average strain at fracture of 2.145%, whereas the strain at fracture for the 0° samples was 2.438%, indicating a 13.7% higher strain at fracture.

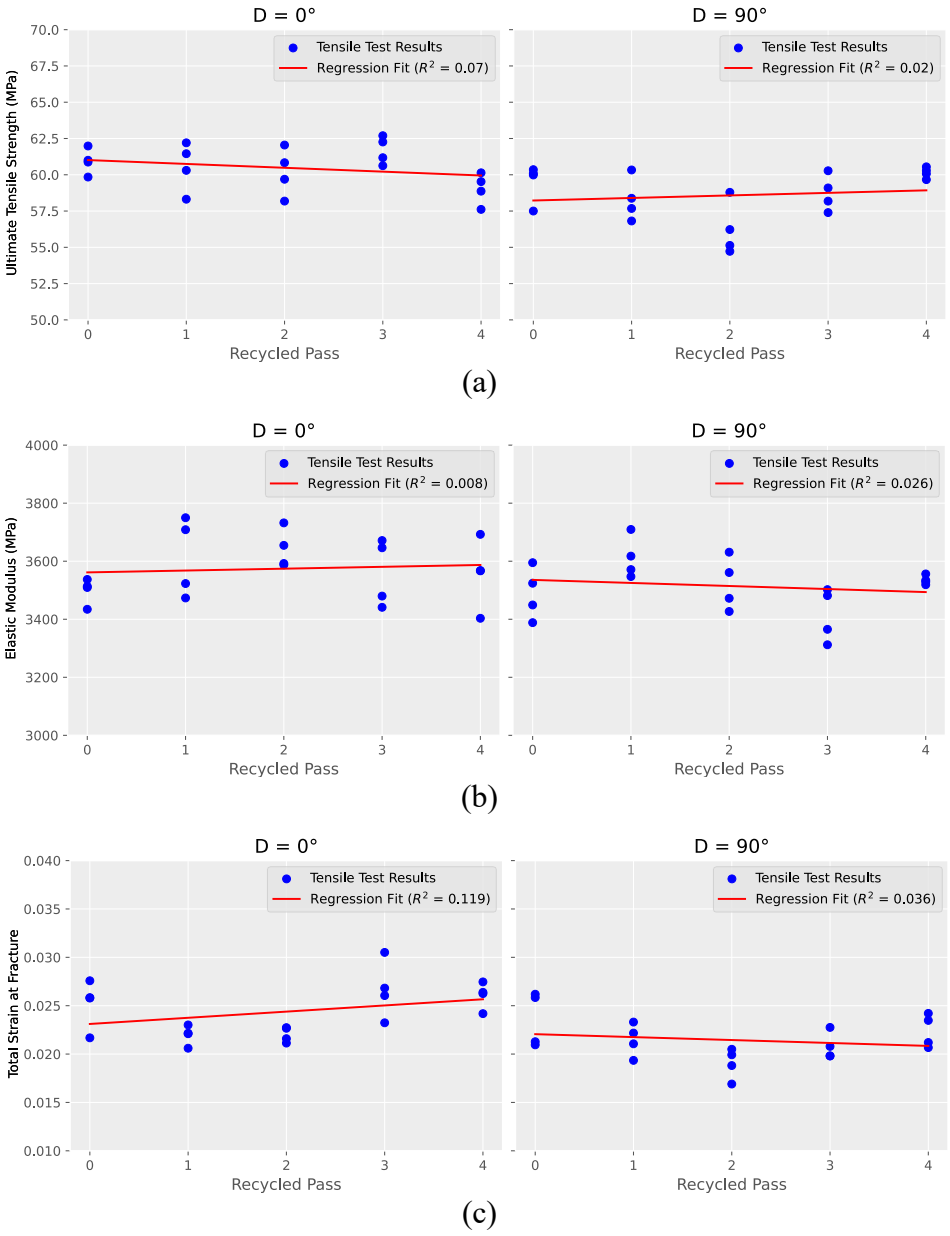

Figure 13: Regression Line over Ultimate Tensile Strength (a), Elastic Modulus (b) and Total Strain at Fracture (c) at 0° and 90°

Referring to Figure 13(a), the samples tested in a 0° orientation exhibited a slight decrease in ultimate tensile strength with respect to recycling pass number. The average ultimate tensile strength of the virgin samples was 60.92 ± 0.87 MPa (2 standard deviation error), which decreased to 59.03 ± 1.08 MPa after undergoing four recycling passes. This represents a 3% reduction in the ultimate strength. There is no definite trend in the results shown in Figure 13 (a, b and c) where the correlation coefficient (R^2) ranged from 0.02 to 0.12. These values suggest a very weak correlation within the dataset, contrary to prior research that generally observed significant differences in ultimate tensile strength between the number of recycling passes. This outcome is unexpected, and the variation from previous literature may be attributed to differences in the method used for sample preparation in our research.

Conclusion

This paper has presented a comprehensive study on benchmarking the tensile properties of polylactic acid (PLA) recycled through the fused granule fabrication additive manufacturing process. The research established a procedure and provided a benchmark dataset for evaluating the mechanical degradation of PLA through multiple recycling passes.

The findings indicate that there is no notable degradation in the mechanical properties of the tensile tested specimens throughout four recycling passes. There is no visible trend evident regarding the elastic modulus or strain at fracture, displaying neither an increase nor a decrease, which was surprising since the expected results should have shown a significant difference in different orientations. However, a decrease of 3% in ultimate tensile strength was observed solely in the case of the 0° orientation. Although the data suggest potential trends, the available experimental data are insufficient to confirm them definitively. Therefore, further investigation is necessary, which could involve conducting additional tests with a larger sample size or considering modifications to the experimental protocol.

The sample geometry of stacked individual beads with bead edges eliminated by machining allowed us to examine the layer-to-layer adhesion and alignment of bead centers in our tests. It is unknown whether our finding that samples pulled in the 0° and 90° orientations displayed comparable mechanical properties would extend to samples including lateral bead edges with the same processing conditions. Many FGF applications use structures with multiple perimeters and nonzero infill, unlike our samples composed of single bead perimeters with no infill, and thus additional testing would be needed to understand mechanical properties of those structures.

In comparing the different recycling passes, we observed that there were no distinct patterns indicating significant degradation. This suggests that the recycling, printing, and milling processes employed in our study do not lead to substantial degradation, even after four recycling passes. These findings indicate that the PLA material used in our study exhibits high recyclability. It is important to note that the controlled experimental conditions we used differ from the real-life conditions that parts may encounter during their usage. Factors such as moisture, UV radiation, chemical attack, bacteria, abrasion, dirt/particles, or contamination with other polymers during recycling can affect the performance and properties of recycled materials. Our study focuses on the optimal scenario for the circular economy, demonstrating that thermoplastics, specifically PLA, can withstand four recycling passes without encountering

significant issues. However, we did observe slight variations in properties from one recycling pass to another. This highlights the stochastic nature of thermal processing and the influence of material history. In our study, the extrusion temperature and duration were carefully controlled to ensure the melting of crystals and restoration of the microstructure to an amorphous state (normalized). Additionally, the passive cooling in our specific part geometry likely prevented significant crystallization. While our research showcases the potential of PLA for multiple recycling passes under controlled conditions, it is important to consider the real-world factors and challenges that may impact the performance and properties of recycled materials. Further studies are needed to explore the impact of environmental factors and real-life usage conditions on the recyclability and performance of thermoplastics.

The benchmark dataset presented in this study provides valuable information regarding the mechanical degradation of PLA through fused granule fabrication additive manufacturing and multiple recycling cycles. The findings emphasize the importance of considering the limitations of recycled PLA materials when designing components for specific applications.

References

[1] F. A. Cruz Sanchez, H. Boudaoud, M. Camargo, and J. M. Pearce, "Plastic recycling in additive manufacturing: A systematic literature review and opportunities for the circular economy," *J Clean Prod*, vol. 264, p. 121602, Aug. 2020, doi: 10.1016/J.JCLEPRO.2020.121602.

[2] H. A. Little, N. G. Tanikella, M. J. Reich, M. J. Fiedler, S. L. Snabes, and J. M. Pearce, "Towards Distributed Recycling with Additive Manufacturing of PET Flake Feedstocks," *Materials 2020, Vol. 13, Page 4273*, vol. 13, no. 19, p. 4273, Sep. 2020, doi: 10.3390/MA13194273.

[3] J. Shah, B. Snider, T. Clarke, S. Kozutsky, M. Lacki, and A. Hosseini, "Large-scale 3D printers for additive manufacturing: design considerations and challenges," *International Journal of Advanced Manufacturing Technology*, vol. 104, no. 9–12, pp. 3679–3693, Oct. 2019, doi: 10.1007/s00170-019-04074-6.

[4] A. L. Woern, D. J. Byard, R. B. Oakley, M. J. Fiedler, S. L. Snabes, and J. M. Pearce, "Fused particle fabrication 3-D printing: Recycled materials' optimization and mechanical properties," *Materials*, vol. 11, no. 8, Aug. 2018, doi: 10.3390/ma11081413.

[5] S. Kaza, L. Yao, P. Bhada-Tata, F. Van Woerden, and K. Ionkova, "What a waste 2.0 : a global snapshot of solid waste management to 2050," p. 272.

[6] A. Ravindran *et al.*, "Open Source Waste Plastic Granulator," *Technologies (Basel)*, vol. 7, no. 4, Dec. 2019, doi: 10.3390/TECHNOLOGIES7040074.

[7] D. J. Byard, A. L. Woern, R. B. Oakley, M. J. Fiedler, S. L. Snabes, and J. M. Pearce, "Green fab lab applications of large-area waste polymer-based additive manufacturing," *Addit Manuf*, vol. 27, p. 515, May 2019, doi: 10.1016/j.addma.2019.03.006.

[8] J. Maris, S. Bourdon, J. M. Brossard, L. Cauret, L. Fontaine, and V. Montembault, "Mechanical recycling: Compatibilization of mixed thermoplastic wastes," *Polym Degrad Stab*, vol. 147, pp. 245–266, Jan. 2018, doi: 10.1016/J.POLYMDEGRADSTAB.2017.11.001.

[9] B. D. S. Deeraj, J. S. Jayan, A. Saritha, and K. Joseph, "PLA-based blends and composites," *Biodegradable Polymers, Blends and Composites*, pp. 237–281, Jan. 2022, doi: 10.1016/B978-0-12-823791-5.00014-4.

[10] D. Moreno Nieto, M. Alonso-García, M. A. Pardo-Vicente, and L. Rodríguez-Parada, "Product Design by Additive Manufacturing for Water Environments: Study of Degradation and Absorption Behavior of PLA and PETG," *Polymers 2021, Vol. 13, Page 1036*, vol. 13, no. 7, p. 1036, Mar. 2021, doi: 10.3390/POLYM13071036.

[11] K. Hamad, M. Kaseem, and F. Deri, "Recycling of waste from polymer materials: An overview of the recent works," *Polym Degrad Stab*, vol. 98, no. 12, pp. 2801–2812, Dec. 2013, doi: 10.1016/J.POLYMDEGRADSTAB.2013.09.025.

[12] M. Cieślik *et al.*, "Multiple Reprocessing of Conductive PLA 3D-Printing Filament: Rheology, Morphology, Thermal and Electrochemical Properties Assessment," *Materials 2023, Vol. 16, Page 1307*, vol. 16, no. 3, p. 1307, Feb. 2023, doi: 10.3390/MA16031307.

[13] D. Tanney, N. A. Meisel, and J. Moore, "Investigating Material Degradation Through the Recycling of PLA in Additively Manufactured Parts," 2017, Accessed: Jun. 06, 2023. [Online]. Available: https://repositories.lib.utexas.edu/handle/2152/89857

[14] I. Anderson, “Mechanical Properties of Specimens 3D Printed with Virgin and Recycled Polylactic Acid,” *3D Print Addit Manuf*, vol. 4, no. 2, pp. 110–115, Jun. 2017, doi: 10.1089/3DP.2016.0054/ASSET/IMAGES/LARGE/FIGURE5.JPEG.
[15] S. Gradinaru *et al.*, “Analysis of the anisotropy for 3D printed pla parts usable in medicine Functional outcomes after surgical treatment of hand fractures: ORIF vs CRIF tehniques View project Separation of hydrogen isotopes by water-hydrogen chemical exchange View project ANALYSIS OF THE ANISOTROPY FOR 3D PRINTED PLA PARTS USABLE IN MEDICINE,” *Bull., Series B*, vol. 81, 2019, [Online]. Available: https://www.researchgate.net/publication/337972918
[16] D. P. Cole *et al.*, “AMB2018-03: Benchmark Physical Property Measurements for Material Extrusion Additive Manufacturing of Polycarbonate,” *Integr Mater Manuf Innov*, vol. 9, no. 4, pp. 358–375, Dec. 2020, doi: 10.1007/s40192-020-00188-y.
[17] Y. Kok *et al.*, “Anisotropy and heterogeneity of microstructure and mechanical properties in metal additive manufacturing: A critical review,” *Mater Des*, vol. 139, pp. 565–586, Feb. 2018, doi: 10.1016/j.matdes.2017.11.021.
[18] “Gigabot X 2 – re:3D | Life-Sized Affordable 3D Printing.” https://re3d.org/portfolio/gigabot-x/ (accessed Jun. 25, 2023).
[19] “LX175 PLA.” https://www.filabot.com/products/lx175-pla (accessed Jun. 25, 2023).